J Opt (July 2025) 54(3):1043–1051
https://doi.org/10.1007/s12596-024-01807-z

RESEARCH ARTICLE

Sensitivity enhancement of biosensor (SPR) with $PtSe_2$ using Au–Si–Au thin films

H. Bouandas[1] · Y. Slimani[2] · K. Ayadi[1] · M. A. Ghebouli[3,4] · A. Djemli[5,6] · M. Fatmi[3] · T. Chihi[3] · Munirah D. Albaqami[7] · Saikh Mohammad[7] · Mika Sillanpää[8,9]

Received: 25 January 2024 / Accepted: 16 March 2024 / Published online: 11 April 2024

Abstract In this study, we presented a novel structure for a highly sensitive surface plasmon resonance (SPR) sensor, we propose a structure which contains six layers: BK7 prism glass, Gold thin film, Silicon sheets, Gold thin film, using transition figure of merit (FOM) 16.43 RUI^{-1}metal dichalcogenides 2D $PtSe_2$ layer and sample medium. We have been optimizing the thickness of each layer. The highly performance parameters in this biosensor structure are provided in terms of sensitivity(*S*), detection accuracy (*DA*), quality factor (*QF*) and figure of merit (FOM). Here, the addition of the hybrid *Silicon—*$PtSe_2$ layer between two gold films increased the sensitivity, but we observed the (*DA*) and (*QF*) is decreased. We find the full at half maximum also decreased. We investigated the effect of gold thickness. The maximum sensitivity *200°/RIU* and is gained with 35 nm Gold film, 5 nm thickness Silicon and 2 nm$PtSe_2$ layer, we can be obtained also the configuration with 60 nm Gold thin film and 3 nm thickness Silicon (6 layer) delivers a maximum sensitivity (S) of *206°/RIU* with figure of merit (FOM) of 24.03 RUI^{-1}.Our novel structure is optimized for a highly sensitive surface plasmon resonance (SPR) sensor.

Keywords Surface plasmon resonance · Thickness optimization · Biosensor · Silicon · PtSe2 · Sensitivity

✉ M. Fatmi
fatmimessaoud@yahoo.fr

1 Applied Optics Laboratory, Institute of Optics and Precision Mechanics, University Ferhat Abbas, Setif 1, 19000 Setif, Algeria

2 Laboratory of Intelligent System, Faculty of Technology, University Ferhat Abbas Setif 1, 19000 Setif, Algeria

3 Research Unit On Emerging Materials (RUEM), University Ferhat Abbas of Setif 1, 19000 Setif, Algeria

4 Department of Chemistry, Faculty of Sciences, University of Mohamed Boudiaf, M'sila 28000, Algeria

5 Faculty of Physics, University of Sciences & Technology Houari Boumediene (U.S.T.H.B), BP 32, 16111 El AliaBab, Ezzouar, Algiers, Algeria

6 Department of physics, Faculty of Sciences, University of Mohamed Boudiaf, M'sila 28000, Algeria

7 Department of Chemistry, College of Science, King Saud University, P.O. Box 2455, 11451 Riyadh, Saudi Arabia

8 Department of Biological and Chemical Engineering, Aarhus University, Norrebrogade 44, 8000 Aarhus C, Denmark

9 Sustainability Cluster, School of Advanced Engineering, UPES, Bidholi, Dehradun, Uttarakhand 248007, India

Introduction

Surface plasmon resonance phenomena occur optically, which achieves more excellent detection sensitivity [1]. Surface plasmons (*SP*) are free quantities of surface oscillations, obtained at the surface of a thin metallic film, the collective charge density oscillations propagate confined to the metallic dielectric interface. When the wave vector of an incident light couples with the wave vector of the evanescent wave, it is called a surface plasmon resonance (SPR) [2, 3]. The prism coupler used by Kretsch Amann's ATR. In this configuration, the base of the prism is directly connected to the metal [4], but in otto's configuration it used a very thin air gap between the prism and the film metal [5], for the purpose of exciting the surface plasmon. *SPR* sensors have received increasing attention due to their recent applications such as nanofibers and photonic crystal fiber [6, 7], solar cells [8], to detect specific bio-sensing [9, 10], used for detecting fat and melamine concentration milk [11]. Detection of chikungunya, virus dengue virus and diagnosis of novel coronavirus SARS-CoV-2 [12–14], designed for cancer cell detection

[15, 16] biochemical interaction and detecting nano-objects in solution [17, 18] including medical diagnosis [19, 20], to detect disease in human teeth [21].

However, the SPR-based sensor is an excellent technique for sensing due to its important advantages such as high sensitivity, faster response, the dynamics of a reaction to follow in real time and the wide range of refractive index of the analyte [22–24]. Although SPR sensors use a variety of materials, recent research is interested in traditional transition metal dichalcogenides (*TDM*), because of their perfect electronic and optical properties. Recently, traditional (TDMs) have been intensively investigated theoretically and experimentally to demonstrate that some noble metals can form a layered structure with S and Se, of which $PtSe_2$ is one of the most important properties, such as the largest band gap of (1,2 eV) for a monolayer of semiconductors, going from a bulk semi-metallic $PtSe_2$ with zero band gap its strong interlayer interaction. On the other hand, the $PtSe_2$ can also offers inertness to chemical agents and resilience to toxicity, making it a suitable material for sensing applications [25].

It found a great advancement of the sensitivity of *SPR* by using the modified schema. These papers are presented as follows, the mathematical expression is in Sect. 2, the results and discussion are discussed in Sect. 3. Finally, the conclusion and necessary references are arranged at the end.

Mathematical background

This proposed structure is a modified Kretschmann model, as shown in Fig. 1. We used an *SPR*sensor using a multilayer composition consisting of a metal (Gold) film deposited at the base of the BK7 glass prism, silicon (Si) is attached with Gold. film, and the exterior of the silicon layer is also kept in direct contact with another metal layer. The biomolecular recognition element consists of the $PtSe_2$ layer, which has a monolayer thickness of 0.375 nm [31].

The refractive index of the biological sample is considered to vary from 1.33 [32]. The BK7 glass prisms is characterized by the following dispersion relation (1) [33]:

$$n_p = \sqrt{\frac{1.03961212\lambda^2}{\lambda^2 - 0.00600069867} + \frac{0.231792344\lambda^2}{\lambda^2 - 0.0200179144} + \frac{1.03961212\lambda^2}{\lambda^2 - 103.560653} + 1} \tag{1}$$

However, Silicon is getting more and more attention last 10 years due to its low cost. The addition of silicon in the structure *SPR* layer is capable of raising its sensitivity [26], Verma et al. used the silicon between the Gold and graphene layer in the *SPR* sensor was the highest sensitivity [27]. Ougang et al. have proposed the structure base for Silicon and *TMDs* on Gold film, and it was achieved with a more excellent sensitivity [28]. Rajeev et al. proposed *SPR*sensor-based Silicon and two-dimensional MXene (Ti_3C_2TX) to increase the sensitivity [29]. The employing of the Si nanomaterials has been theoretically improved the sensitivity [15]. $PtSe_2$ over Ag and Au has demonstrated significant for improving sensitivity of sensor up to 162 deg/RIU and 265 deg/RIU, respectivity. Rahman et al. are designed a novel structure (Ag–$PtSe_2$–WSe_2) there sensitivity are 194 deg/RIU and 187 deg/RIU, respectively [30]. M. Mahabubur et *al*. have been proposed (Au–WSe_2–$PtSe_2$–BP) for improving the sensitivity up to 200 deg/RIU [31]. In this context of the present paper, we propose the traditional *SPR* biosensor schema based six layers on Silicon-$PtSe_2$ coated biosensor. It was introduced in order to analyze and characterize some keys such as change of resonance angle θ_{res}, minimum reflectance (R_{min}), FWHM, detection accuracy (*DA*), sensitivity (*S*) and *FOM*. We suggest a novel structure used numerical simulations of transfer matrix method (TMM); Here the architect-based Au/Si/Au/$PtSe_2$ explored to improve its sensitivity.

where λ the wavelength (μm).

The complex RI of Gold at different wavelengths can be calculated from the Drude-Lorentz model [34]:

$$\varepsilon_G = 1 - \frac{\lambda^2 \lambda_c}{\lambda_p^2(\lambda_c + i\lambda)} \tag{2}$$

Here $\lambda_c = 2.4511 \times 10^{-5} m$ and $\lambda_p = 1.6826 \times 10^{-7} m$ are the collusion and the plasma wavelength of Gold,

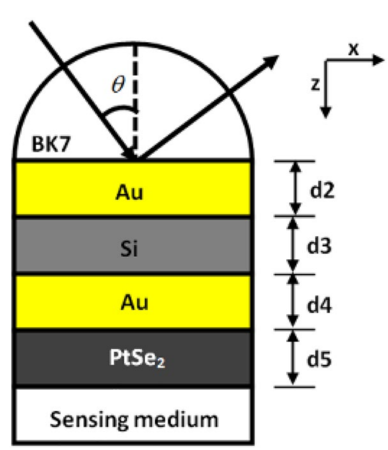

Fig. 1 Multilayer stack diagram of the biosensor based on *Si* and $PtSe_2$

respectively. The Silicon layer refractive index can be calculated using the following equation [35].

$$n_{Si} = A + A_1 e^{-\lambda t_1} + A_2 e^{-\lambda t_2} \tag{3}$$

where: $A = 3.44904$, $A_1 = 2271.88813$, $A_2 = 3.39538$, $t_1 = 0.058304$ and $t_2 = 0.30384$ at λ wavelength in µm. The complex dielectric value of $PtSe_2$ dependents on the thickness at wavelength of 633 nm, it is calculated using from the literature [36, 37].

We employ the matrix method to calculate the reflectance of the reflected light of the six-layer model. This matrix method is efficient and does not require any approximation. In this structure, all the layers are structured in the Z direction, each layer is characterized by the thickness (dk) and the constant optics of the metal and the dielectric. The relation between the tangential components of the electric field (E) and the tangential components of the magnetic fields (H) at the first and the final layer is given by [38].

$$M = \prod_{G=2}^{G-1} M_G = \begin{bmatrix} M_{11} & M_{12} \\ M_{21} & M_{22} \end{bmatrix} \tag{4}$$

$$M_G = \begin{bmatrix} cos\delta_G & \frac{-sin\delta_G}{q_G} \\ -iq_G sin\delta_G & cos\delta_G \end{bmatrix} \tag{5}$$

where η_G is the phase factor of the thin film and δ_G is the phase thickness and is determined as:

$$q_G = \frac{\sqrt{n_G^2 - k_G^2 - n_p^2 sin^2\theta_i - 2in_G k_G}}{\varepsilon_G} \tag{6}$$

$$\delta_G = \frac{2\pi}{\lambda} d_G \sqrt{n_G^2 - k_G^2 - n_p^2 sin^2\theta_i - 2in_G k_G} \tag{7}$$

θ_i is the angle of incidence, and n_G,k_G are constant optic of the complex refractive index and d_G the thickness of the metal layer.

$$r_p = \frac{(M_{11} + M_{12} q_N) q_1 - (M_{21} + M_{22} q_N)}{(M_{11} + M_{12} q_N) q_1 + (M_{21} + M_{22} q_N)} \tag{8}$$

The reflectance (R) is given by:

$$R_p = \left| r_p \right|^2 \tag{9}$$

Results and discussion

The optimization of sensitivity, detection accuracy and quality factor were considered as the main performance parameters of the excellent SPR sensor. The sensitivity (S) can be defined as the ratio of the change in the resonance angle (θ_{SPR}) to the change in the refractive index of the sensing region:

$$S = \frac{d\theta_{SPR}}{dn_{biosample}} \tag{10}$$

The detection accuracy (DA) is a known as the ratio of the shift resonance angle (θ_{SPR}) to the full width at half maximum of the resonance plasmon curve as can be seen in the following relation:

$$DA = \frac{1}{FWHM} \tag{11}$$

Another important parameter of interest is the figure of merit (FOM) that is determine as the ratio of the reflectance curve of sensitivity to the $FWHM$ [39]:

$$FOM = \frac{S}{FWHM} \tag{12}$$

Three schematic structure and their performance parameters of the SPR sensor reflectance curve for each structure as a function of the incident angle of sensing medium summarized in Table 1.

Figure 2a; show the movement of resonance angle is 1° with small increment in $RI = 0.005$ for$d(Au) = 35$ nm, d(Si) = 5 nm. It can see the calculated sensitivity from Eq. (10) of conventional sensor is *200°/RIU*; after increasing thickness of Gold and decreasing thickness of silicon d(Au) = 60 nm, d(Si) = 3 nm in conventional SPR sensor. It can observe that the sensitivity achieved *206°/RIU* shown in Fig. 2b.

Table 2; presents the values of minimum reflectance (R_{min}), sensitivity (S), full width half maximum ($FWHM$), detection accuracy (DA), and figure of merit (FOM) at the

Table 1 Performance parameters of SPR sensor reflectance curve for different structure

Sensor structure used	R_{min}	Sensitivity (°RIU^{-1})	FWHM (°)	DA ($°^{-1}$)	FOM (RIU^{-1})
BK7/Au/sensing medium	0.2693	142	2.48	0.4032	57.25
BK7/Au/$PtSe_2$ /sensing medium (15)	0.3515	165	11.68	0.1412	14.12
BK7/Au/Si/Au/$PtSe_2$ /sensing medium	0.0254	200	12.17	0.082	16.43

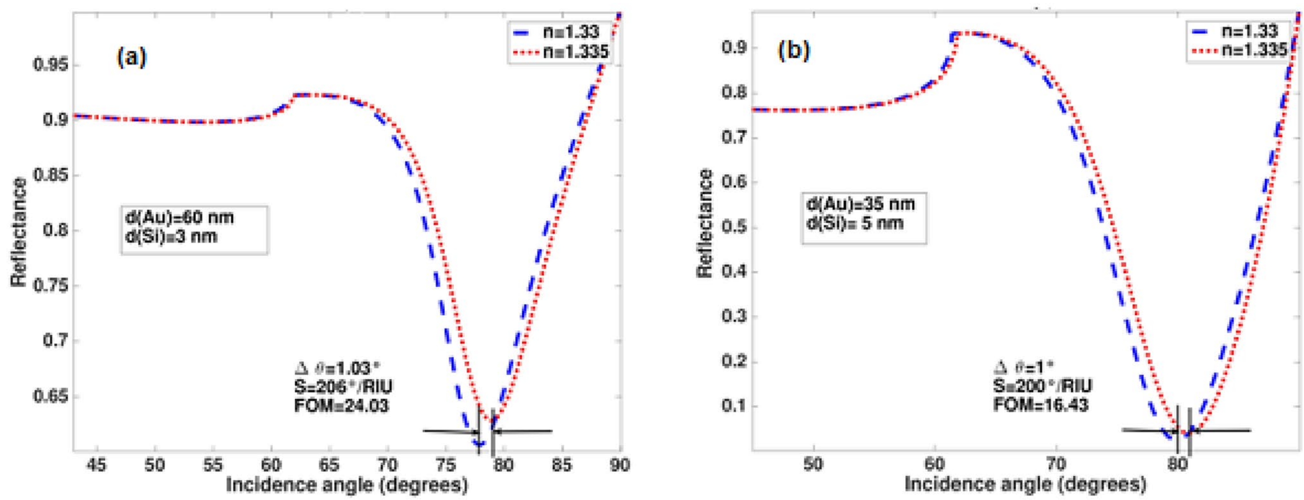

Fig. 2 Reflectance curve as a function of the incident angle for d(Au) = 35 nm, d(Si) = 5 nm (**a**) and d(Au) = 60 nm, d(Si) = 3 nm (**b**)

Table 2 Performance parameter for optimized combination of Gold and Si thickness of proposed SPR

d(*Au*)	d(*Si*)	d($PtSe_2$)	R_{min}	S	FWHM	DA	FOM
35	5	0	0.099	178	5.48	0.182	32.48
60	5	0	0.375	234	8.37	0.119	27.95
35	0	2	0.005	144	8.31	0.120	17.32
60	0	2	0.531	166	5.77	0.173	28.76
35	3	2	0.026	176	10.80	0.092	16.29
60	3	2	0.606	206	8.57	0.116	24.03
35	5	2	0.025	200	12.17	0.082	16.43
60	5	2	0.725	116	9.95	0.100	11.65

wavelength 633 nm. the optimization thickness of Gold (*Au*), Silicon (*Si*) and the thickness of ($PtSe_2$) at the illustrated in Fig. 3a–f. It can be observed from Table 2 that the high sensitivity and FOM of the two conventional structure $Au/Si/Au/PtSe_2$ for combination (1) with thickness Au(35 nm)/Si(5 nm)/Au(5 nm)/$PtSe_2$(2 nm), combination (2) and combination (3) Au(60 nm)/Si(5 nm)/Au(5 nm)/$PtSe_2$(2 nm), for the best combination of SPR biosensor proposed is the structure having Au(60 nm)/Si(5 nm)/Au(5 nm)/$PtSe_2$(2 nm) its property optimum highest sensitivity, optimum figure of merit *206°/RIU* and 24.03 respectively. However, the sensitivity, R_{min} and *DA* values for combination (1) are *200°/RIU*, 0.025 and 0.082, respectively. It can be seen in Table 2; that when adding Si layer in the configuration Kretchmann without PtSe2 layer the sensitivity achieved 234°/RIU, this means adding Si layer on sandwich Gold is sufficient to increase the sensitivity enhancement, but biochemical detection needs to use Si and PtSe2 which greatly allow one to detect analyte.

In this work, the main aim was to optimize the thickness of ($PtSe_2$), we plotted the change in resonance angle and the minimum reflectivity with various thickness of Silicon sheets (3, 5 and 7 nm) and the thickness of gold film (30, 35, 40, 45, 50 and 60 nm). Figure 3a–c and d–f show the simulation results of the ($\Delta\theta_{res}$) and (R_{min}) respectively.

From Fig. 3a–c we have compared its (Δθres), it found at the thickness of (PtSe2) equal to 2 nm the ($\Delta\theta_{res}$) is as great as for 35 nm thickness of Gold and 5 nm thickness of Silicon ($\Delta\theta_{res} = 1°$) and it can be seen from the plot is the highest that 60 nm thickness of Gold and 3 nm thickness of Silicon ($\Delta\theta_{res} = 1.03°$).

Similarly, Fig. 3d–f shows the minimum reflectivity curves for different thickness of (Gold) with optimized thickness of layer ($PtSe_2$), and for Fig. 3e at 35 nm thickness of Gold and with 632 nm wavelength, it can be observed from these plots that minimum reflectivity is lower for this case and for Fig. 3d at 60 nm thickness of Gold, it is clear that the minimum reflectivity is still very highest ($R_{min} = 0.60$) which indicates that the SPR in this structure is not strong and the sensing medium is not very remarkable. For a perfect biosensor, ($\Delta\theta_{res}$) should be high, but at the moment (R_{min}) should be minimum.

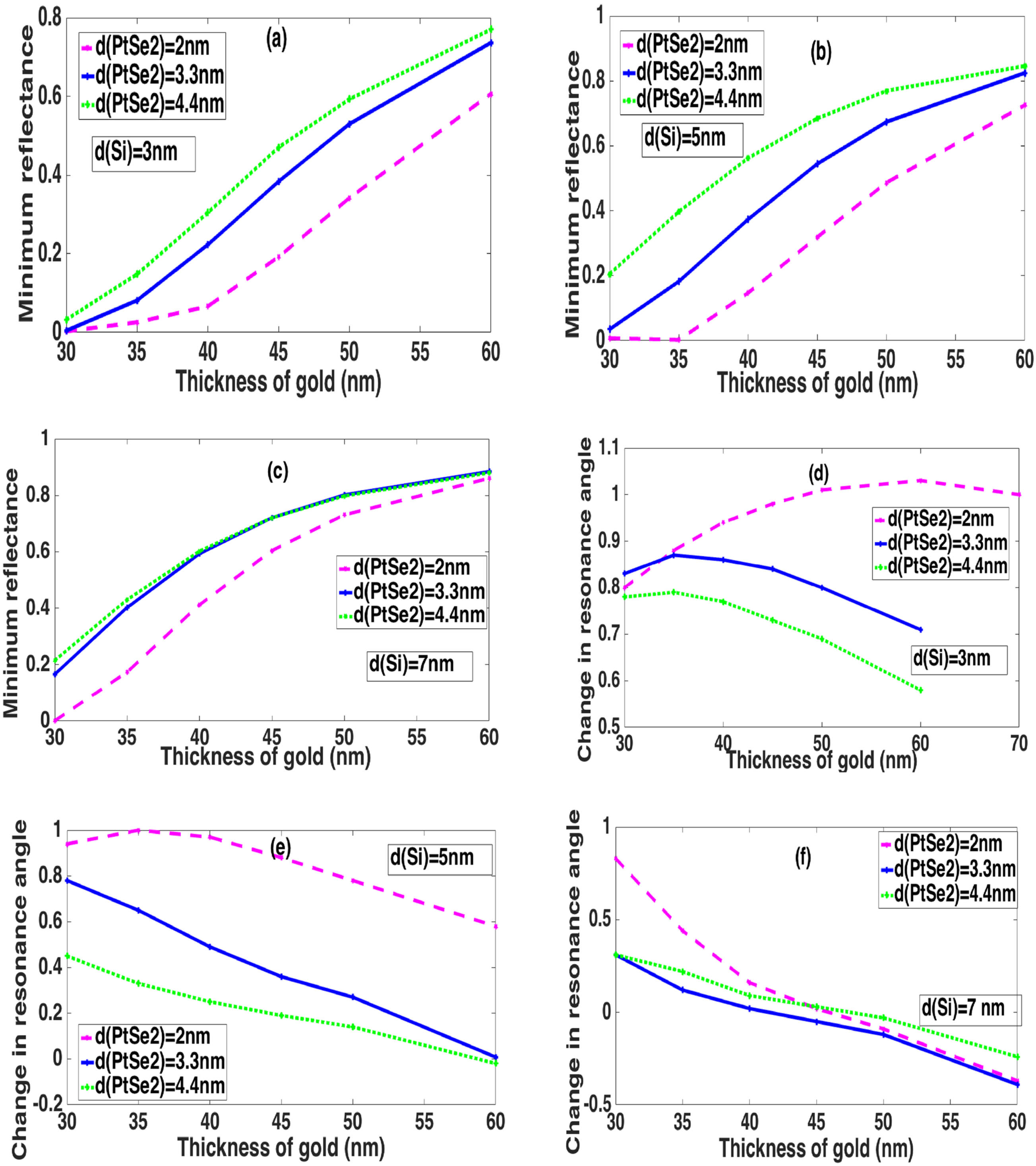

Fig. 3 Minimum reflectivity (R_{min}) resonance angle ($\Delta\theta_{res}$) as a function variation of the thickness of Gold for 2, 3.3, and 4.4 nm of PtSe2 at Si 3, 5, 7 nm

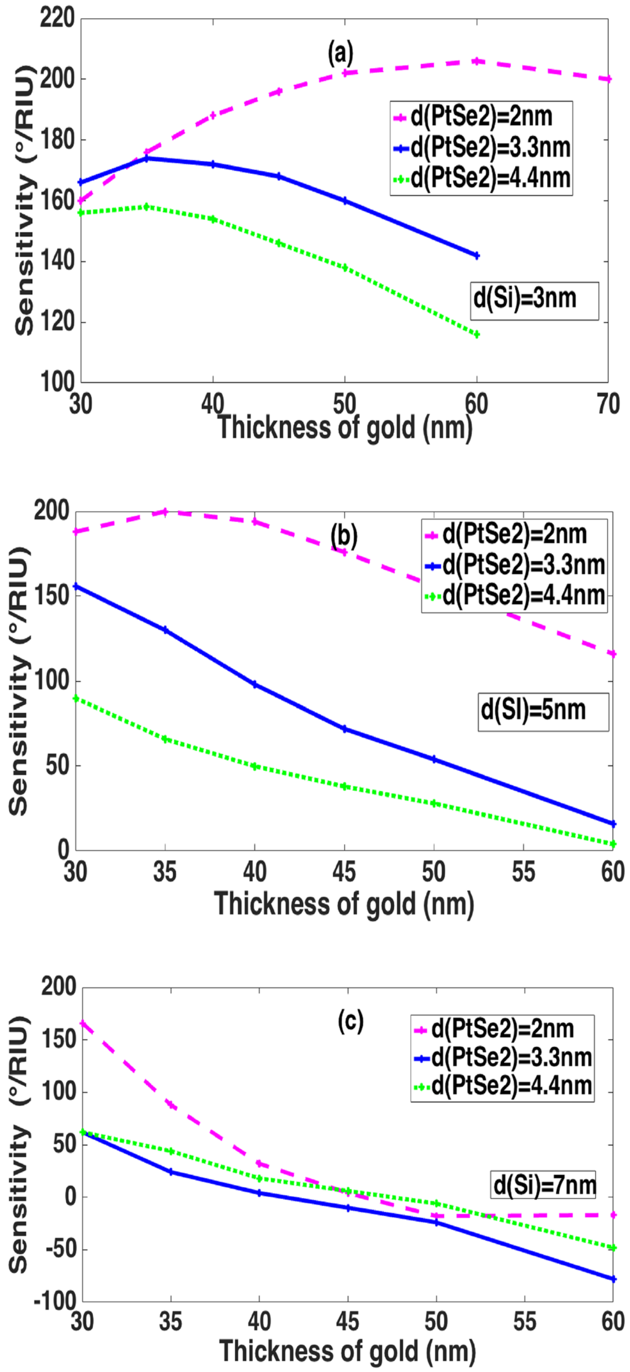

Fig. 4 The sensitivity as a function thickness of Gold and different thicknesses of $PtSe_2$with **a** d(Si) = 2 nm, **b** d(Si) = 5 nm and **c** d(Si) = 7 nm a wave length 632.8 nm

From Fig. 4, the result shows that change of sensitivity. First, the sensitivity is quasi linear decreasing with the lowest thickness ($PtSe_2$).

The Fig. 4a shows, the sensitivity varies at 60 nm thickness of Gold to *S = 206°/RIU* with thickness of d($PtSe_2$) = 2 nm at S = *142°/RIU* with thickness of d($PtSe_2$) = 4.4 nm. We may therefore conclude that the sensitivity is best at the lowest (PtSe2) thickness. Secondly, the result illustrates that the sensitivity increased with increasing of gold thickness at 3 nm thickness of Silicon and at the thickness of d($PtSe_2$) = 2 nm.

We can achieve for Fig. 4b at d($PtSe_2$) = 2 nm the sensitivity increase at the maximum d(Au) = 35 nm equal to *200°/RIU* and then decreases.

Another important parameter for study a *SPR* biosensor is detection accuracy (*DA*), it is highest for lower thickness ($PtSe_2$), we can see for Fig. 5a the (*DA*)increase with increase of thickness of Gold at d($PtSe_2$) = 2 nm. From Fig. 5b show the (*DA*) increase for maximum and started to decrease.

We calculated the *FOM* by the formula *FOM* = S/FWHM. From this, we can get the *FOM* increase with the increase of thickness of Gold showing a Fig. 6a. For Fig. 6b the *FOM* decrease with the increase of thickness of ($PtSe_2$).

Table 3; shows the comparison among the enhancement of the proposed *SPR* sensor with another existing *SPR* sensor in the literature, and has information on the sensitivity, minimum reflectance, and quality factor at the 633 nm wavelength.

Conclusion

In this study, we have theoretically investigated a novel *SPR* biosensor using (with insertion of) a Silicon layer and $PtSe_2$ layer of the conventional structure to obtain better performances. In this proposed *SPR* biosensor working on the visible light region by using the transfer matrix method. The structure is based on six layers, in which first is a low refractive index BK7as the coupling prism and insertion the silicon layer and $PtSe_2$ layer between two gold films. The changes of different architect parameters are improving the sensitivity. It found that the change of resonance angle decreases on increasing the thickness of $PtSe_2$. and the present analysis also represents that the *FWHM* decreases up to the extent due to which the quality factor and detection accuracy improve enormously. The result demonstrated that the maximum sensitivity as high as *200°/RIU* with figure of merit (FOM) 16.43 RUI^{-1}can achieved with structure is designed for gold (35 nm), Silicon (5 nm) and $PtSe_2$ (2 nm), where the highest sensitivity *206°/RIU* can be obtained for Gold (60 nm), Silicon (3 nm) and $PtSe_2$ (2 nm). Additionally, the maximum figure of merit (FOM) is 16.43 RUI^{-1}.

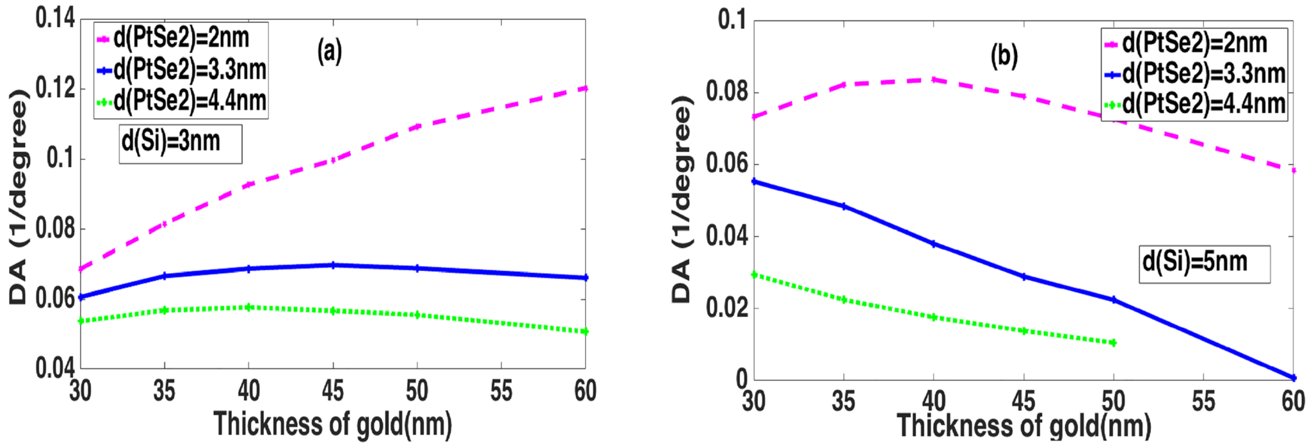

Fig. 5 The *DA* as a function thickness of Gold d(Si) = 3 nm (**a**) and d(Si) = 5 nm (**b**)

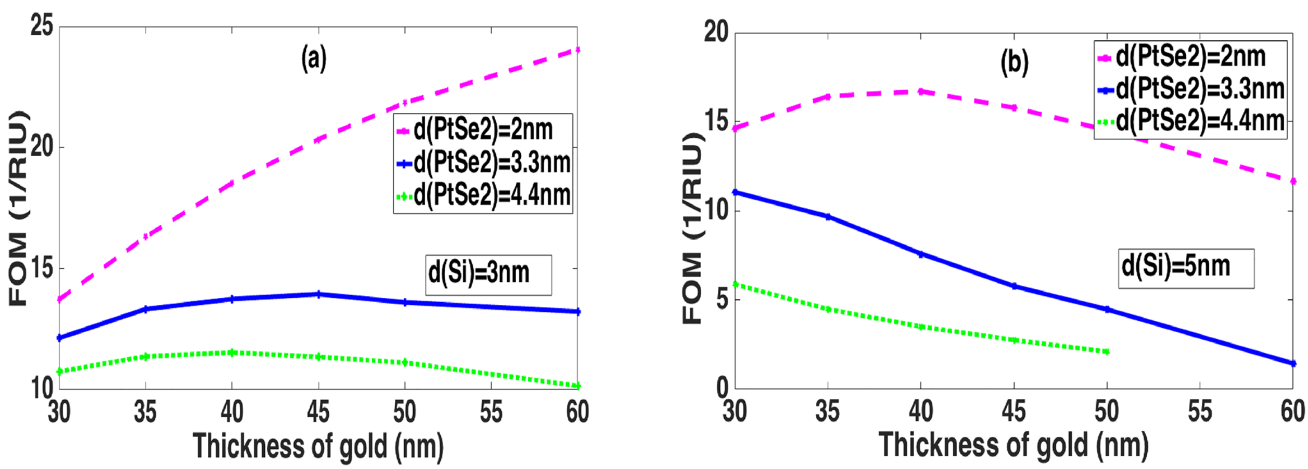

Fig. 6 The *FOM* as a function thickness of Gold d(Si) = 3 nm (**a**) and d(Si) = 5 nm (**b**)

Table 3 Comparison of proposed work with another existing sensor

Ref	Enhancement strategy				
	λ (nm)	S (°/RIU)	Rmin	QF (RIU^{-1})	FOM (RIU^{-1})
Xu et al. [40]	633	156	–	–	–
Srivastava et al. [41]	633	190	0.0692	15.51	–
Wu et al. [41]	633	160	–	–	–
Jia et al. [42]	633	165	0.3515	14.12	–
Rikta et al. [43]	633	96.43	–	12.36	–
Rahman et al. [31]	633	200	0.2554	–	17.70
kumar et al. [44]	633	174.1	–	–	–
Villarmi et al. [17]	633	85.5	–	–	–
Karki et al. [45]	633	161	–	11.89	81.32
Rahman et al. [30]	633	194	–	34	–
Proposed work	633	200	0.0254	0.0822	16.43
Proposed work	633	206	0.6068	0.0815	24.03

It is expected that the novel structure may be very much useful in different fields of biosensing and optical sensing application.

Acknowledgements This work was funded by the Researchers Supporting Project Number (RSP2024R267) King Saud University, Riyadh, Saudi Arabia.

Authors contributions statements Conceptualization, Data curation: H. Bouandes. Formal analysis, Methodology: M.A. Ghebouli, M. Fatmi. Software: A. Djemli, Visualization, Validation, Writing—review & editing: Y. Slimani. Roles/Writing—original draft: K. Ayadi, M. Fatmi, Munirah D. Albaqami, Saikh Mohammad and Mika Sillanpaa, T. Chihi.

Declaration

Conflict of interests The authors declared no potential conflicts of interest with respect to the research, authorship, and/or publication of this article.

References

1. M. Pirzada, Z. Altintas, Recent progress in optical sensors for biomedical diagnostics. Micromachines **11**(4), 356 (2020)
2. S. A. Maier. Plasmonics: fundamentals and applications. Springer Science & Business Media, Cham (2007).
3. H. Reather, Surface plasmons on smooth and rough surfaces and on gratings. Tracts Modern Phys. **111**, 1–3 (1988)
4. E. Kretschmann, The determination of optical constants of metals by excitation of surface plasmons. Z. Phys. **241**, 313–324 (1971)
5. A. Otto, Excitation of nonradiative surface plasma waves in silver by the method of frustrated total reflection. Z. Phys. A: Hadrons Nucl. **216**(4), 398–410 (1968)
6. E.K. Sobolewska, A. Laghrissi, T. Kawalec, L. Jozefowski, H. Rubahn, J. Adam, J. Fiutowski, Para-hexaphenylene (p-6p) nanofibersgrown on asilver surface for polarization-insensitive surface plasmonpolariton excitation. Opt. Commun. **511**, 127995 (2022)
7. T. Dai, J. Yan, W. Zhu, L. Bian, Z. Yi, M. Liu, Z. Yu, Ultra-high sensitivity surface plasmon U-channel photonic crystal fiber for hemoglobin sensing. Sens. Actuators, A **366**, 115053 (2024)
8. K. Dutta, A. Datta, S. Majumder, Design of plasmonic solar photocatalyst: judicially coupled hot carrier induced surface plasmon of Ag with graphene. Opt. Mater. **123**, 111887 (2022)
9. A. Asad, H.S. Khaliq, A. Zahid, M.Q. Mehmood, Y. Massoud, Uniform chirality enhanced optical responses via broadband achiral metasurfaces for bio-sensing applications. Nanophotonics, Micro/Nano Optics, and Plasmonics VIII. In: Proc. SPIE, vol 12322, pp 56–61 (2022)
10. P. Das, A. Gupta, M. Maruthapandi, A. Saravanan, S. Srinivasan, A. R. Rajabzadeh, A. Gedanken, Polymer composites for biosensors. In: Polymeric Nanocomposite Materials for Sensor Applications. Woodhead Publishing, UK, pp 323–342 (2023).
11. L. Fatolahi, S. Alemi, M.N. Al-Delfi, A.H. Athab, B.J. Janani, Optical detection of fat and adulterants concentration milk using TMDC (WS2 and MoS2)-surface plasmon resonance sensor via high sensitivity and detection accuracy. Opt. Mater. **147**, 114723 (2024)
12. T.I. Singh, P. Singh, B. Karki, Early detection of chikungunya virus utilizing the surface plasmon resonance comprising a silver-silicon-PtSe2 multilayer structure. Plasmonics **18**(3), 1173–1180 (2023)
13. B. Karki, N.H. Salah, G. Srivastava, A. Muduli, R.B. Yadav, A simulation study for dengue virus detection using surface plasmon resonance sensor hetero structure of silver, barium titanate, and cerium oxide. Plasmonics **18**(6), 2031–2040 (2023)
14. T.B.A. Akib, S. Mostufa, M.M. Rana, M.B. Hossain, M.R. Islam, A performance comparison of heterostructure surface plasmon resonance biosensor for the diagnosis of novel coronavirus SARS-CoV-2. Opt. Quant. Electron. **55**(5), 448 (2023)
15. N.H. Salah, A. Pal, H.M. Rasul, A. Uniyal, Sensitivity enhancement of the surface plasmon resonance sensor based on gallium-doped zinc oxide and silicon for cancer detection: a wavelength interrogation approach. Micro Nanostruct. **186**, 207736 (2024)
16. S. Singh, A.K. Sharma, P. Lohia, D.K. Dwivedi, V. Kumar, P.K. Singh, Simulation study of reconfigurable surface plasmon resonance refractive index sensor employing bismuth telluride and MXene nanomaterial for cancer cell detection. Phys. Scr. **98**(2), 025813 (2023)
17. M.R. Villarim, D.R. Belfort, C.P. de Souza, A Surface Plasmon Resonance (SPR)-Based Biosensor Simulation Platform for Performance Evaluation of Different Constructional Configurations. Coatings **13**(3), 546 (2023)
18. Q. M. Al-Bataineh, A. D. Telfah, C. J. Tavares, R. Hergenröder, Modeling and analysis of discrete particle detection in wide-field surface plasmon resonance microscopy. Sensors Actuators A: Phys. 115266 (2024).
19. T. Fatima, S. Bansal, S. Husain, M. Khanuja, Biosensors. In Electrochemical Sensors. Woodhead Publishing, UK, pp 1–30 (2022).
20. G. I. Janith, H. S. Herath, N. Hendeniya, D. Attygalle, D. A. S. Amarasinghe, V. Logeeshan, Y. S. Wijayasinghe, Advances in surface plasmon resonance biosensors for medical diagnostics: an overview of recent developments and techniques. J. Pharmaceutical Biomed. Anal. Open, 100019 (2023).
21. M. K. Alam, V. Dhasarathan, A. Natesan, R. Nambi, M. U. Zaman, K.K. Ganji, H, Abutayyem, Human teeth disease detection using refractive index-based surface plasmon resonance biosensor. Coatings, **12**(10), 1398 (2022).
22. H. Bouandas, H. Chorfi, K. Ayadi, Study of human colorectal mucosa by SPR biosensor using admittance loci method. Optik **225**, 165809 (2021)
23. R. Narayanaswamy, O.S. Wolfbeis, J. Homola, Surface plasmon resonance biosensors for food safety. Optical Sensors, 145–172 (2004).
24. J. Homola, S.S. Yee, G. Gauglitz, Surface plasmon resonance sensors. Sens. Actuators, B Chem. **54**(1–2), 3–15 (1999)
25. Y. Jia, Z. Li, H. Wang, M. Saeed, H. Cai, Sensitivity enhancement of a surface plasmon resonance sensor with platinum diselenide. Sensors **20**(1), 131 (2020)
26. J.B. Maurya, Y.K. Prajapati, V. Singh, J.P. Saini, R. Tripathi, Performance of graphene–MoS_2 based surface plasmon resonance sensor using silicon layer. Opt. Quant. Electron. **47**(11), 3599–3611 (2015)
27. R. Verma, B.D. Gupta, R. Jha, Sensitivity enhancement of a surface plasmon resonance-based biomolecules sensor using graphene and silicon layers. Sensors Actuators B: Chem. **160**(1), 623–631 (2011)
28. Q. Ouyang, S. Zeng, L. Jiang, L. Hong, G. Xu, X. Dinh, J. Qian, S. He, J. Qu, P. Coquet, Sensitivity enhancement of transition metal dichalcogenides/silicon nanostructure-based surface plasmon resonance biosensor. Sci. Rep. **6**(1), 28190 (2016)
29. R. Kumar, S. Pal, Y.K. Prajapati, J.P. Saini, Sensitivity enhancement of MXene based SPR sensor using silicon: theoretical analysis. SILICON **13**, 1887–1894 (2021)

30. M.M. Rahman, M.M. Rana, M.S. Rahman, M.S. Anower, M.A. Mollah, A.K. Paul, Sensitivity enhancement of SPR biosensors employing hetero structure of PtSe2 and 2D materials. Opt. Mater. **107**, 110123 (2020)
31. M.M. Rahman, L.F. Abdulrazak, M. Ahsan, M.A. Based, M.M. Rana, M.S. Anower, S. Gurusamy, 2D nanomaterial-based hybrid structured (Au-WSe 2-PtSe 2-BP) surface plasmon resonance (SPR) sensor with improved performance. IEEE Access **10**, 689–698 (2021)
32. S. Pal, A. Verma, Y.K. Prajapati, J.P. Saini, Influence of black phosphorous on performance of surface plasmon resonance biosensor. Opt. Quant. Electron. **49**(12), 403 (2017)
33. E. D. Palik. Handbook of optical constants of solids. Academic Press, New York, vol **3**, (1998).
34. S. Pal, Y. K. Prajapati, J. P. Saini, and V. Singh. Sensitivity enhancement of metamaterial-based surface plasmon resonance biosensor for near infrared. Optica Appl. **46**(1) (2016).
35. S. Ghosh, M. Ray, Analysis of silicon-based surface Plasmon Resonance Sensors with different amino acids. SILICON **7**(4), 313–322 (2015)
36. Z. Cheng, Z. Wang, D.E. Gillespie, C. Lausted, Z. Zheng, M. Yang, J. Zhu, Plain silver surface plasmon resonance for microarray application. Anal. Chem. **87**(3), 1466–1469 (2015)
37. Z. Wang, Z. Cheng, V. Singh, Z. Zheng, Y. Wang, S. Li, L. Song, J. Zhu, Stable and sensitive silver surface plasmon resonance imaging sensor using trilateral metallic structures. Anal. Chem. **86**(3), 1430–1436 (2014)
38. F.Abeles, Recherches sur la propagation des ondes électromagnétiques sinusoïdales dans les milieux stratifies-Application aux couches minces. Ann. de Physique,**12**, 596–640. (1950).
39. S. Pal, Y.K. Prajapati, J.P. Saini, Influence of graphene's chemical potential on SPR biosensor using ZnO for DNA hybridization. Opt. Rev. **27**(1), 57–64 (2020)
40. Y. Xu, Y.S. Ang, L. Wu, L.K. Ang, High sensitivity surface plasmon resonance sensor based on two-dimensional MXene and transition metal dichalcogenide: a theoretical study. Nanomaterials **9**(2), 165 (2019)
41. A. Srivastava, A. Verma, R. Das, Y.K. Prajapati, A theoretical approach to improve the performance of SPR biosensor using MXene and black phosphorus. Optik **203**, 163430 (2020)
42. L. Wu, Q. You, Y. Shan, S. Gan, Y. Zhao, X. Dai, Y. Xiang, Few-layer Ti3C2Tx MXene: A promising surface plasmon resonance biosensing material to enhance the sensitivity. Sensors Actuators B:Chem. **277**, 210–215 (2018)
43. K.A. Rikta, M.S. Anower, M.S. Rahman, M.M. Rahman, SPR biosensor using SnSe-phosphorene heterostructure. Sensing Bio-Sensing Res. **33**, 100442 (2021)
44. V. Kumar, S. Pal, Tantalum disulfide (TaS 2) based novel surface plasmon resonance sensor with enhanced sensitivity using aluminium arsenide (AlAs) and thallium bromide (TlBr). In: 2023 International Conference on Computer, Electronics & Electrical Engineering & their Applications (IC2E3). IEEE, New York, pp 1–6 (2023).
45. B. Karki, B. Vasudevan, A. Uniyal, A. Pal, V. Srivastava, Hemoglobin detection in blood samples using a graphene-based surface plasmon resonance biosensor. Optik **270**, 169947 (2022)

Publisher's Note Springer Nature remains neutral with regard to jurisdictional claims in published maps and institutional affiliations.